



# Design of continuous variable curvature roll shape and straightening process research for two-roll straightener of bar

Lidong Ma<sup>1,2</sup> · Yukang Du<sup>1</sup> · Zijian Liu<sup>1</sup> · Lifeng Ma<sup>1,2</sup>

Received: 11 March 2019 / Accepted: 1 October 2019 / Published online: 14 November 2019  
© Springer-Verlag London Ltd., part of Springer Nature 2019

## Abstract

At present, high straightness precision and good bar surface quality are difficult to meet at the same time in the straightening process of bar. In view of this problem, this paper puts forward a continuous variable curvature roll shape design method, and studies the straightening process setting method. The roll shape of the straightening roll is tangentially connected by multiple segments arc of uniform curvature changes, and the curvature decreases uniformly from the middle to both ends. The roll shape designed by this method can be in good contact with the bar and can effectively improve the surface quality of the straightened bar. In order to make the straightening process parameters more reasonable and effective, reduce the dependence of the production line on workers, and realize the full automatic straightening of the bar, a complete process straightening bending springback model of bar was established. Based on roll shape and bar specification, the optimization iteration model of upper and lower straightening roll angle is established. Then the setting method of the roll gap and the guide plate spacing is discussed. The field straightening process is simulated by finite element analysis. The process setting model is verified on the straightener after roll shape modification. The automatic control of two-roll straightening of bar can be effectively realized by using the roll shape and process model. The straightened bar has high straightness and surface quality.

**Keywords** Straightening · Bar · Two roll · Variable curvature roll shape · Parameters of process

## 1 Introduction

Straightening is an important process of bar finishing line. Flat roll or multi-roll straightening and pressure straightening is difficult to achieve all-around straightening. Only both rotating and forward of the diagonal roll straightening method can achieve this goal. Typical bar straighteners have the seven-roll straightener and the two-roll straightener. Based on the constraint of its roll shape, the two-roll straightener can achieve continuous reverse bending and springback and no blind area or small blind area straightening. The multi-roll straightener can achieve continuous bending and springback of the bar in

the roll system through the joint action of multiple groups of rolls, and there is an inevitably blind area. Existing production practice shows that the two-roll straightener can achieve higher straightening precision. At present, the design method of two-roll straightener mainly focuses on the selection of the bending curvature of the roll shape curve. Masgilleson [1], a scholar from the former Soviet put forward the design method of single curvature roll shape. In the design of roll shape, the curve of roll shape is an arc of equal radius. On the plane section of the bar axis, the straightening roll shape presents the feature of variable curvature, but the feature of curvature change is fixed. Cui [2] put forward a method for the design of three-section curvature roll shape; that is, in the plane section of the bar axis, the curvature at the entrance of the roll shape curve is composed of three sections of arc from small to large, and the measured curvature at the exit of the roll shape curve is composed of three sections of arc from large to small. The curvature of the arc is determined by the plastic deformation of the bar during bending. A longer and uniform straightening method can ensure good surface quality and straightening quality. Pei et al. [3] used a piecewise linearized elastic-plastic stress-strain relation, and the bending straightening

✉ Lidong Ma  
mald@tyust.edu.cn

<sup>1</sup> Coordinative Innovation Center of Taiyuan Heavy Machinery Equipment, Taiyuan University of Science and Technology, Taiyuan 030024, China

<sup>2</sup> Key Laboratory of Metallurgical Equipment Design Theory and Technology of Shanxi Province, Taiyuan University of Science and Technology, Taiyuan 030024, China

process of both side-cut and flat-cut D-type cross-section shaft is modeled and deduced as a straightening prediction model. Three-point parabola method and parabolic fitting method are both proposed for the curvature conversion in the straightening process. Wu et al. [4] studied systematically the straightening process of a bar in a two cross-roll straightener. A mathematical model on the precision of the straightened bars is developed. Yu et al. considered the deformation hardening, Baushinger effect, and cyclic softening; the reciprocating bending springback process is analyzed by using the graphic method. The conclusion showed that the reciprocating bending eliminates the difference of initial curvatures and makes the curvatures be in the same direction and have same value. They also proposed the speed of curvature unification is determined mainly by the ratio of plastic modulus to elastic modulus. The greater the ratio of plastic modulus to elastic modulus is, the slower the speed of curvature uniformity is, and the more the bending time required, then established the equation of residual curvature and the unified equation of residual curvature. It is proved that although the initial curvature of each section of bar is different, the difference of initial curvature is eliminated by the reciprocating bending, and the process mechanism of the two-roll straightening is revealed [5–7]. Lu et al. [8] used the mathematical model of load stroke in the pressure straightening process under the elastic-plastic theory to carry out tests and numerical simulation, and proposed the straightening stroke prediction formula based on the precision straightening stroke deflection model. Wang et al. [9, 10], aiming at the low efficiency of three-point bending straightening, proposed a new three-roll continuous straightening method. Based on the detected deflection data, a piecewise fitting algorithm with constraints by introducing the Kuhn-Tucker condition is proposed for straightness calculation, and a simple polynomial fitting method with fourth order is determined for the calculation of curvature and straightening moment. Then based on the minimum work principle, an analytical model of the cross-sectional distortion of the curved pipe with initial curvature in the reverse axial elastic-plastic bending is established, and the prediction error is not more than 10% compared with the experimental value of the maximum distortion coefficient. Zhao [11] studied the plane bending springback equation with small curvature. And Yin [12] proved that this theory can adapt to the needs of straightening process. Liu et al. [13] studied the straightening process of shape steel by using the curvature integral method, and deduced the method to calculate the residual stress. Zhang [14–16] studied the curvature radius model of thin-walled tube straightening by using the elastic-plastic theory and the classical unloading theory, and studied the flattening phenomenon of section in the straightening process of thin-walled tube by using the energy method. The main technological parameters in bar straightening production include roll gap, straightening roll tilt angle, and guide plate spacing. Zhao et al. [17]

proposed a multi-point bending one-time straightening control strategy that discretizes and linearizes the theoretical bending moment curve. Moon et al. [18] applied finite element method to analyze the residual stress of bar straightening, and believed that the roll gap had significant influence on the residual stress, while the tilt angle of the straightening roll had little influence on it. Ma et al. [19] studied the neutral layer migration theory in the two-roll straightening process, and based on this, they established the equation for solving the residual curvature. Jindřich et al. [20] used the Euler method and the classical Lagrangian method to describe the longitudinal deformation and the transverse deformation respectively. By the above method, they realized the numerical computation of skew roll straightening process. They believe that online prediction and control of process parameters are expected to be realized. Yu [6] started from the research on the technological mechanism of two-roll straightening, and understood the deformation of the bar macroscopically by exploring the deformation path of the bar in the roll gap. Li [21, 22] presented a new inspection algorithm based on local annular contrast (LAC) for steel bar surface defects. Experimental results show that the proposed algorithm needs only 13 ms to inspect one steel bar surface image and its detection accuracy exceeds 95%. Subsequently, it was proposed a lower envelope Weber contrast (LEWC) recognition algorithm to detect steel bar surface pit defects.

In this paper, the design method of roll shape with variable curvature is proposed. The curvature of roll shape curve of straightening roll increases uniformly from one end to the maximum at the waist position, and then gradually decreases to the other end. The curve on both sides of the roll waist is symmetrical. The characteristic of this method is the uniform change of curvature on the roll shape curve, which can eliminate the effect of sudden curvature change on bar bending deformation. Through the effective continuous bending springback theory of rotary straightening process verified by the field, the straightening process of straightening roll of roll shape curve with different curvature range was calculated, the evolution process of each curvature was obtained, and the influence of variable curvature range on the straightening precision of bar was studied. The roll shape designed by this method is verified by numerical simulation. Under the constraint of roll shape, the micro-beam section on the bar can achieve continuous bending and springback; therefore, the relationship between the tilt angle of straightening roll and the reverse bending curvature is studied. The tolerance range and the optimal contact mode of bar products can be used as the setting basis for the parameters of roll gap. Based on elastic-plastic bending springback theory, a quantitative analytical model of the curvature of bar straightening process is established. On this basis, the value of tilt angle is solved iteratively, and the process parameter setting model of bar straightening was established. The straightness and surface

quality of bar are analyzed by finite element analysis. At the same time, the above model is verified by experiments. The results show that the variable curvature roll shape and its process settings can meet the requirements of two-roll straightening of bar and achieve high straightening accuracy and surface quality.

## 2 Design method of continuous variable curvature roll shape

Suppose that the maximum curvature of the variable curvature range is  $K_{\max}\rho_t$  and the minimum curvature is  $K_{\min}\rho_t$ , where  $\rho_t$  is the elastic limit curvature. The position of maximum curvature is the waist of the roll, and the position of minimum curvature is the end. Since the roll is symmetrical on both sides with the waist as the center, only half of the roll is calculated when calculating the roll.  $N$  points are selected from the uniform distance of half the roll, and the axial position of any point is  $z_i$ , ( $i = 1, 2, \dots, n$ ). And since the length of roll profile is generally 8 times the lead( $8t$ ), that is, half of the length of roll profile is 4 times the lead( $4t$ ), then the curvature of any point is

$$\rho_i = \left( \rho_{\min} + \frac{(\rho_{\max} - \rho_{\min})}{4t} z_i \right) \rho_t$$

In this paper, it mainly uses the spatially closed stereo analytic geometry principle and vector relationship, and combines the roll gap shape to derive the corresponding mathematical model. Through computer programming, various roll-type designs can be realized.

The convex roll is discussed first. As shown in Fig. 1, given the curvature of  $n$  segments, each radius of curvature is denoted as  $\rho_i$  ( $i = 1, 2, \dots, n$ ) and the center of curvature is respectively  $O'_i$ . The bar can be regarded as a ring. In Fig. 1, the intersection point between the connecting line from each section to the center of curvature and the center connecting line  $OO'$  of the roll and the bar is  $O_i$ . The distance from  $O_i$  to the bar center at the waist of the roll, and the distance to the bar center corresponding to each roll section are respectively  $Q_i$  and  $L_i$ . The normal line passes the contact area roll face and the bar surface also passes through connected lines formed by their axes  $q_i p_i$ . Let the length of each vector be  $Op_i = e_i$ ,  $mp_i = c_i$ ,  $O'q_i = b_i$ ,  $Om_i = f_i$ ,  $R_0 + r = h$ , where  $R_0$  is the waist radius of the straightening roll,  $r$  is the bar radius, and  $h$  is the distance between the bar center and the center of the straightening roll at the waist position of the roll

From closed vector relations,

$$h + b_i + r_i + c_i = e_i$$

$$h + b_i + r_i = f_i$$

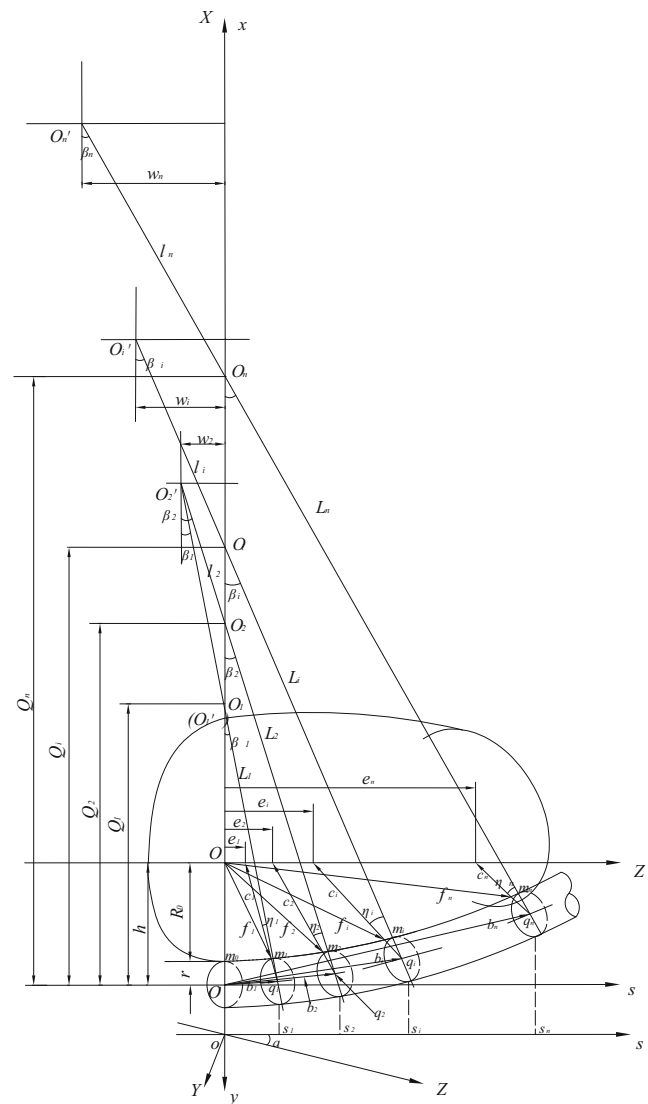


Fig. 1 Spatial geometry of contact between bar and convex roll

In the OXYZ coordinate system, the component form of each vector is

$$h = [-h, 0, 0]$$

$$b_i = [Q_i - L_i \cos \beta_i, -L_i \sin \beta_i \sin \alpha, L_i \sin \beta_i \cos \alpha]$$

$$r_i = \left[ r \cos \varphi_i \cos \beta_i, r (\sin \varphi_i \cos \alpha + \cos \varphi_i \sin \beta_i \sin \alpha), r (\sin \varphi_i \sin \alpha - \cos \varphi_i \sin \beta_i \cos \alpha) \right]$$

$$c_i = \left[ c_i \cos \varphi_i \cos \beta_i, c_i (\sin \varphi_i \cos \alpha + \cos \varphi_i \sin \beta_i \sin \alpha), c_i (\sin \varphi_i \sin \alpha - \cos \varphi_i \sin \beta_i \cos \alpha) \right]$$

$$e_i = [0, 0, e_i]$$

$$f_i = [X_i, Y_i, Z_i]$$

where  $\alpha$  is the angle between the bar and the center line of the straightening roll projected on the horizontal plane;  $\beta_i$  is the angle between  $\rho_i$  and the vertical center line of the roll waist position;  $\phi_i$  is the angle between  $\rho_i$  and  $p_i q_i$ ; and  $X_i$ ,  $Y_i$ , and  $Z_i$  are the coordinate value of the contact point  $m_i$ .

From  $e_i$  known  $e_{ix} = 0$ , the closed vector expression is

$$h_x + b_{ix} + r_{ix} + c_{ix} = 0$$

That is

$$-h + Q_i - L_i \cos \beta_i + (c_i + r) \cos \phi_i \cos \beta_i = 0 \quad (1)$$

From  $e_i$  known  $e_{iy} = 0$ , the closed vector expression is

$$h_y + b_{iy} + r_{iy} + c_{iy} = 0$$

That is

$$-L_i \sin \beta_i \sin \alpha + (C_i + r)(\sin \phi_i \cos \alpha + \cos \phi_i \sin \beta_i \sin \alpha) = 0 \quad (2)$$

By  $f_{ix} = X_i$ , we can get

$$h_x + b_{ix} + r_{ix} = x_i$$

That is

$$X_i = -h + Q_i - L_i \cos \beta_i + r \cos \phi_i \cos \beta_i \quad (3)$$

By  $f_{iy} = Y_i$  we can draw

$$Y_i = -L_i \sin \beta_i \sin \alpha + r(\sin \phi_i \cos \alpha + \cos \phi_i \sin \beta_i \sin \alpha) \quad (4)$$

By  $f_{iz} = Z_i$  we can draw

$$Z_i = -L_i \sin \beta_i \cos \alpha + r(\sin \phi_i \cos \alpha - \cos \phi_i \sin \beta_i \sin \alpha) \quad (5)$$

It can be obtained from Formula (1) and Formula (2)

$$\tan \phi_i = \frac{(Q_i - h) \sin \beta_i \tan \alpha}{h - Q_i + L_i \cos \beta_i}$$

That is

$$\phi_i = \arctan \frac{(Q_i - h) \sin \beta_i \tan \alpha}{h - Q_i + L_i \cos \beta_i} \quad (6)$$

It can be known from the position and plane geometry of the bar in Fig. 1.

$$\beta_i = \arcsin \left[ \frac{w_i + z_i}{\rho_i} \right]$$

$$Q_1 = L_1 = \rho_1$$

$$w_i = (\rho_i - L_{i-1}) \sin \beta_{i-1}$$

$$l_i = w_i / \sin \beta_{i-1}$$

$$Q_i = Q_{i-1} + \frac{w_i}{\tan \beta_{i-1}} - \frac{w_i}{\tan \beta_i}$$

$$L_i = \rho_i - l_i$$

Then press set  $\rho_i$ ,  $\alpha$  and  $h$  to get

$$\beta_i = \arcsin \left[ \frac{(\rho_i - L_{i-1}) \sin \beta_{i-1} + z_i}{\rho_i} \right] \quad (7)$$

$$Q_i = Q_{i-1} + (\rho_i - L_{i-1}) \left( \cos \beta_{i-1} - \frac{\sin \beta_{i-1}}{\tan \beta_i} \right) \quad (8)$$

$$L_i = \rho_i - (\rho_i - L_{i-1}) \frac{\sin \beta_{i-1}}{\sin \beta_i} \quad (9)$$

The initial value is substituted with  $i = 1$  when calculating. And known  $\beta_0 = 0$ ,  $L_0 = 0$ , and  $Q_0 = 0$ , we can calculate the points  $Q_i$ ,  $L_i$ , and  $\varphi_i$ , then the coordinate values  $X_i$ ,  $Y_i$ , and  $Z_i$  are obtained. And we obtained the roll radius  $R_i$  at the roll axis coordinate  $Z_i$  is

$$R_i = \sqrt{X_i^2 + Y_i^2} \quad (10)$$

The concave roll of the one-way reverse bending straightening roll is a roll pressed against the outer arc side of the workpiece, the contact point  $m_i$  of the workpiece and the roll surface are turned from the inner arc side to the outer arc side, and each space vector is also changed from the inner arc side to the outer arc side. The positive direction of the vector is consistent with the positive direction of  $X$ ,  $Y$ , and  $Z$ . The angle is positive with a depression angle and negative with an elevation angle. The radius of curvature  $\rho_i$  of each segment and its associated line segments ( $L_i$ ,  $l_i$ ,  $Q_i$ ) are positive when they are above the bar axis  $Oz$ , and negative when they are below the bar axis  $Oz$ ; that is,  $L_i$ ,  $Q_i$ ,  $\sin \beta_i$  and  $\rho_i$  are negative. Substituting it into Formulas (3)–(10) can be used to calculate a set of concave roll shape calculation formula.

The flow chart of the variable curvature roll shape is shown in Fig. 2. It can be seen that in calculating the roll shape curve, the smaller the pitch  $\Delta z$ , the more points taken on the roll shape curve, the better the continuity of the drawn roll shape, and the smoother the roll surface of the straightening roll.

Figure 3 shows the basic structural parameter calculation software interface. The blue in the lower right corner is the partial curve of the concave roll shape, and the green is the partial curve of the convex roll shape (the roll shape fillet is not drawn in the interface, and the roll spacing parameter is temporarily not applied).

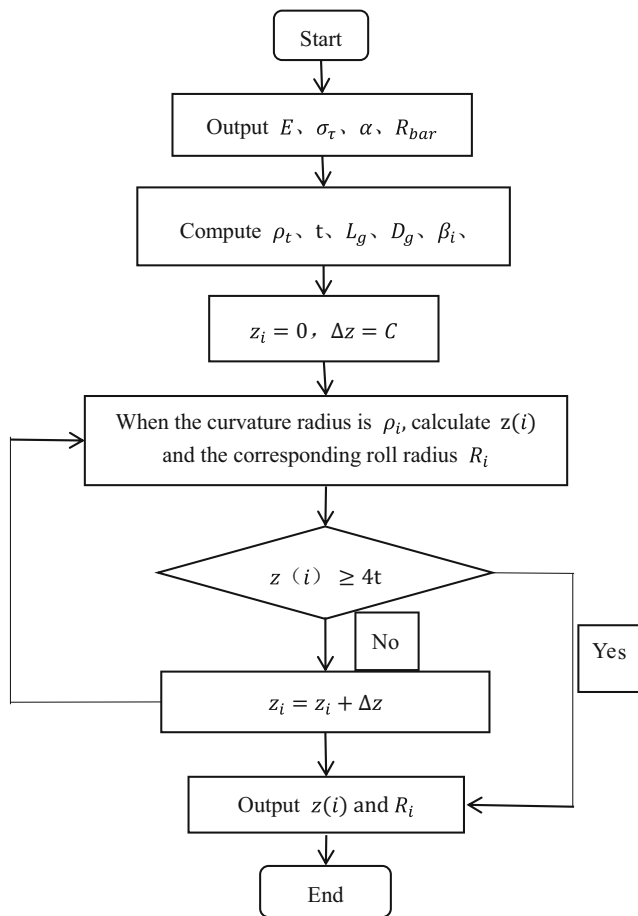


Fig. 2 Roll-type calculation flow chart

### 3 Full process bending springback theory of straightening process

Bar bending springback process satisfies the curvature equation, that is,

$$K_p = K - K_f \tag{11}$$

where  $c$  is the residual curvature,  $K$  is the reverse bending curvature,  $K_f = \frac{M}{EI}$  is the springback curvature,  $E$  is the elastic modulus of the bar,  $I$  is the moment of inertia of the bar section, and  $M$  is the bending moment, which can be obtained by integrating the moment balance in the bending state.

Set the bar diameter to  $R$ . When the micro-beam section is bent from the original curvature  $K_0$  to the curvature  $K$ , the strain is  $\varepsilon$  and the stress is  $\sigma$ . In the geometric center layer coordinate system, the ordinate of any point on the section of the bar is  $z$ , and the distance from the elastic-plastic boundary point to the neutral layer is  $z_E$ .

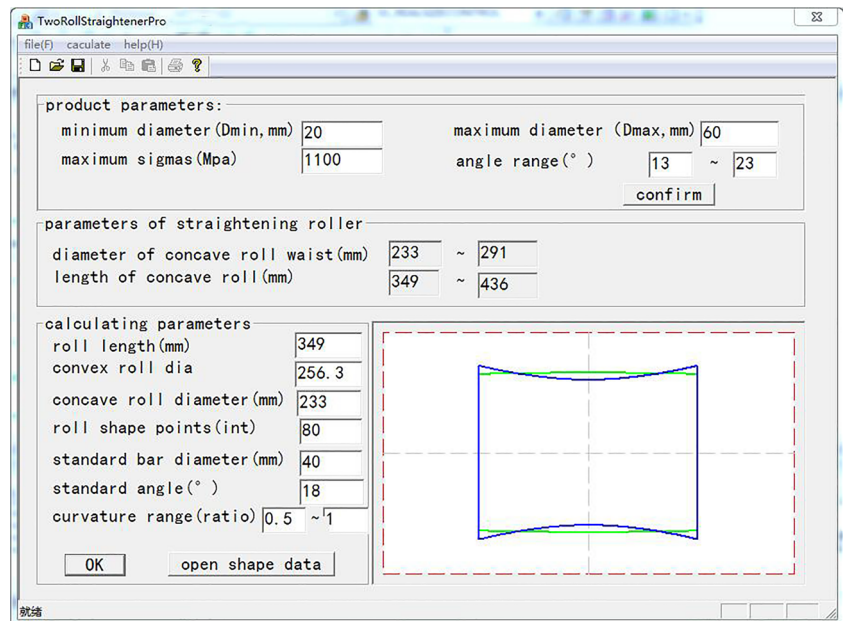
$$\varepsilon = z(K - K_0) \tag{12}$$

$$z_E = \frac{\sigma_s}{E|K - K_0|} \tag{13}$$

$$\theta_E = \arcsin \frac{z_E}{R} = \arcsin \frac{\sigma_s}{E|K - K_0|R} \tag{14}$$

As shown in Fig. 4, for the case where the symmetrical section is purely curved, to calculate the bar bending moment, simply integrate the quarter of the section coordinates and multiply by 4. Under this premise, the bending moment when the bar is purely bent is divided into the following two cases.

Fig. 3 Basic structure parameter calculation software interface





When  $z_E \geq R$ , bar section is pure elastic deformation.

$$M = \int_A \sigma z dA = \int_A E z^2 (K - K_0) dA = E(K - K_0) \iint_A z^2 dy dz$$

$$= \frac{\pi E (K - K_0) R^4}{4} \tag{15}$$

When  $0 < z_E < R$ , the bar occurs elastic deformation, and demarcation point is at  $z_E$ .

$$M = 4 \int_A \sigma z dA = 4 \int_0^{z_E} E z^2 (K - K_0) dA + 4 \int_{z_E}^R (D\varepsilon + \sigma_0) z dA$$

$$= 4 \int_0^{z_E} E z^2 (K - K_0) dA + 4 \int_{z_E}^R \left[ Dz(K - K_0) + 4\sigma_s \left( 1 - \frac{D}{E} \right) \right] z dA$$

$$= 4E(K - K_0) \int_0^{z_E} \int_0^{\sqrt{R^2 - z^2}} dy \int_0^{z_E} z^2 dz + 4D(K - K_0) \int_0^{\sqrt{R^2 - z^2}} dy \int_{z_E}^R z^2 dz + 4\sigma_s \left( 1 - \frac{D}{E} \right) \int_0^{\sqrt{R^2 - z^2}} dy \int_{z_E}^R z dz$$

$$= 4E(K - K_0)L1 + 4D(K - K_0)L2 + 4\sigma_s \left( 1 - \frac{D}{E} \right) L3 \tag{16}$$

where,

$$L1 = \int_0^{z_E} z^2 \sqrt{R^2 - z^2} dz = \int_0^{\arcsin(\frac{z_E}{R})} R^2 \sin^2 \theta R^2 \cos^2 \theta d\theta$$

$$= \frac{R^4}{8} \left[ \arcsin \frac{z_E}{R} - \frac{\sin 4 \left( \arcsin \frac{z_E}{R} \right)}{4} \right]$$

$$L2 = \int_{z_E}^R z^2 \sqrt{R^2 - z^2} dz = \int_{\arcsin(\frac{z_E}{R})}^{\frac{\pi}{2}} R^2 \sin^2 \theta R^2 \cos^2 \theta d\theta$$

$$= \frac{R^4}{8} \left[ \frac{\pi}{2} - \left( \arcsin \frac{z_E}{R} - \frac{\sin 4 \left( \arcsin \frac{z_E}{R} \right)}{4} \right) \right]$$

$$L3 = \int_{z_E}^R z \sqrt{R^2 - z^2} dz = -\frac{1}{2} \int_{z_E}^R (R^2 - z^2)^{\frac{1}{2}} d(R^2 - z^2)$$

$$= \frac{1}{3} (R^2 - z_E^2)^{\frac{3}{2}}$$

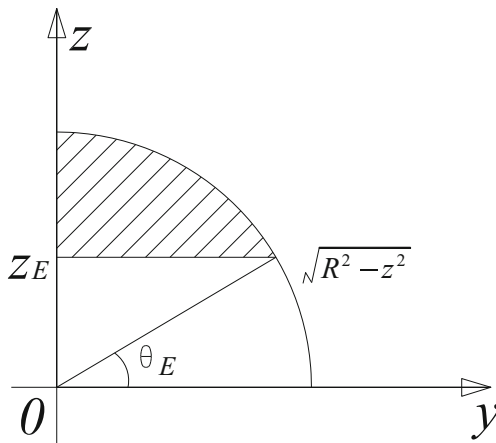


Fig. 4 Bar cross-section integral diagram

When  $K$  and  $K_0$  are known, the bending moment can be calculated according to Formula (16), and then substituted into the curvature equation  $K_p = K - K_f$  to calculate the residual curvature after the second turn.

As shown in Fig. 5, the bar rotates forward in the roll system, and the micro-unit  $abcd$  on the bar is transferred to the two-point  $a, b$  position from two points  $c(a'), d(b')$  after the bar rotates half a turn, and the two points  $c, d$  are rotated to the position  $c', d'$ . The segment  $ab$  is transformed from being stretched to compressed, and the segment  $cd$  is converted from compressed to stretched; that is, the microcell achieves a reverse bend.

The lead  $t$  is the distance that the bar passes in the straightening direction for one revolution. The distance that the bar has passed through one reverse bending is  $t/2$ .

$$t = \pi d \tan \alpha \tag{17}$$

where  $t$  is the lead;  $d$  is the diameter of the bar;  $\alpha$  is the angle between the straightening roll and the bar.

Assume that the initial deflection of the bar is  $s_0$  ( $\text{mm} \cdot \text{m}^{-1}$ ), then the initial curvature can be calculated according to the following formula.

$$K_0 = \frac{2s_0}{500 \times 500 + s_0 \times s_0} \tag{18}$$

After the bar is stably straightened, the bending state of the bar in the concave roll and the convex roll is stable, and the bending state is considered to be a state in which the bar is subjected to the reverse bending during the bending process. The curvature of each point on the contact line between the concave roll and the

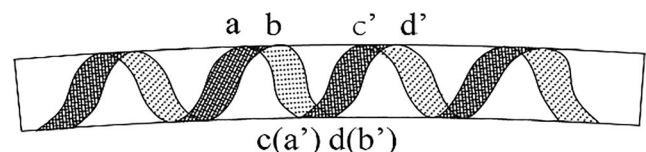


Fig. 5 Schematic diagram of rotary reverse bending

bar is taken as the bending curvature of the bar. The contact line can approximately take the intersection line between the vertical surface of the bar axis and the concave roll. The approximate solution of the curvature is as follows.

As shown in Fig. 6, the straight line  $MN$  is the projection line of the vertical plane passing through the bar axis on the horizontal surface of the concave roll. The lower circle is the section circle of the position corresponding to any point  $A$  on the straight line, and the point  $A'$  is the corresponding point of the point  $A$  on the section circle. The vertical direction is the  $z$  direction, the direction of the roll waist is the  $x$  direction, and the vertical direction of the section circle is the  $y$  direction. The angle between the bar axis and the straightening roll axis is  $\alpha$ . A point  $z$  direction coordinate is  $z_i$ , and the coordinates of the point  $A$  in the

$x$  direction and  $y$  direction are defined as  $x_i$  and  $y_i$ . If the roll radius corresponding to the point  $A$  is  $R_i$ , the relationship is

$$\begin{aligned} x_i &= z_i \cdot \tan \alpha \\ x_i^2 + y_i^2 &= R_i^2 \end{aligned}$$

From  $z_i$ ,  $R_i$ , and  $\alpha$ , you can calculate  $x_i$  and  $y_i$  by calculating the coordinates of each point on the intersection line between the vertical surface of the bar and the straightening roll. The curve function  $y = f(x)$  of the intersection line can be obtained by fitting the spline function, and the bending curvature  $K_i$  at any point can be calculated by the following formula.

$$K_i = \frac{|y_i''|}{(1 + y_i'^2)^{3/2}} \tag{19}$$

The bending moment of the  $i$ th bending is defined as  $M_i$  and the bending moment  $M_1$  can be obtained after the steel tube with initial curvature of  $K_0$  passes through the first point of reverse bending (reverse bending curvature  $K_{f1}$ ), so as to obtain the springback curvature  $K_{f1}$  of the first reverse bending and the residual curvature  $K_{p1}$  after the first bending. Then the steel tube enters the next bending, and the residual curvature  $K_{(i-1)}$  serves as the initial curvature of the next bending. The iteration equation of residual curvature after resilience of the  $i$ th bending can be obtained from Eq. (1). The integrated result is shown in Formula (20).

$$K_{pi} = \begin{cases} K_i \pm \frac{M_i(K_i, K_0)}{EI} & i = 1 \\ K_i \pm \frac{M_i(K_i, K_{p(i-1)})}{EI} & i \geq 2 \end{cases} \tag{20}$$

According to the above equation programming, the residual curvature after each bending can be obtained, and the final residual curvature (the final straightening accuracy) can be obtained.

### 4 Effect of curvature range on straightening accuracy

According to the roll shape calculation scheme, the most important part of the roll shape calculation is to give the variable curvature range. Different ranges of curvature are used to straighten the bars of the parameters shown in Table 1.

For the sake of understanding, the project gives the curvature range in the form of the radius of curvature, and the bar's elastic limit radius of curvature is  $\rho_t$ . The ranges of curvature radius given are  $1\rho_t \sim 0.2\rho_t$ ,  $1\rho_t \sim 0.3\rho_t$ ,  $1\rho_t \sim 0.5\rho_t$ ,  $1\rho_t \sim 0.7\rho_t$ , and  $0.7\rho_t \sim 0.2\rho_t$ , where

$$\rho_t = \frac{Ed}{2\sigma_t}$$

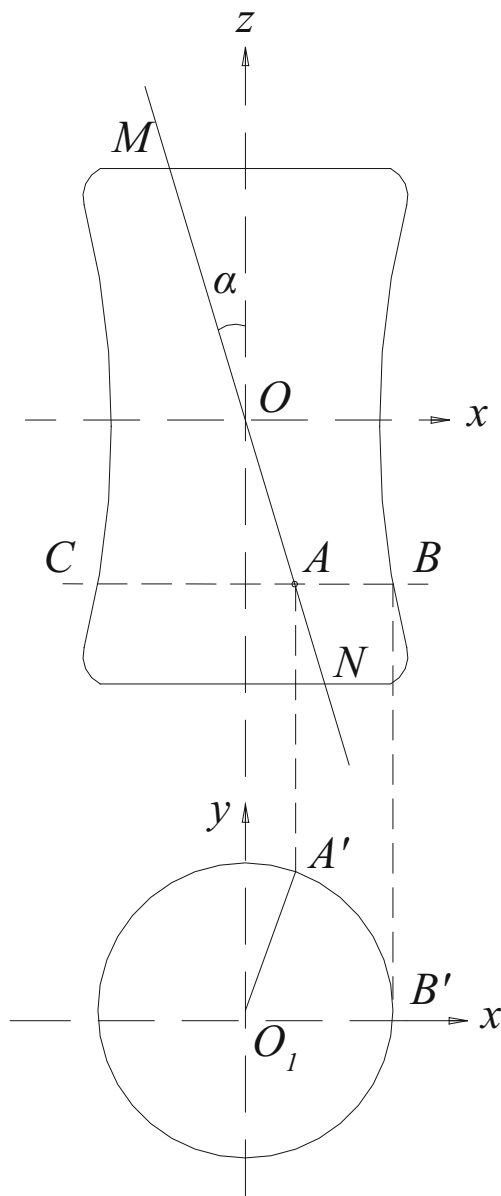


Fig. 6 Schematic diagram of bending curvature analysis

**Table 1** Straightening-related parameters

Bar diameter/mm	Bar yield strength/MPa	Material elastic modulus/MPa	Material hardening modulus/MPa	Original deflection/(mm/m)	Straightening roll angle/°	Roll length/mm
40	800	210000	50000	10	10	400

Figures 7, 8, 9, 10, and 11 show the original curvature, inverse bending rate, elastic curvature, and residual curvature evolution process of the above cases of variable curvature range.

The following conclusions can be drawn from Figs. 7, 8, 9, 10, and 11:

- (1) Different curvature variation ranges can straighten the same bar. The difference is that the various curvatures are different during the bending springback process. Under the same original curvature, the larger the inverse bending curvature, the larger the springback curvature is. The residual curvature experience becomes smaller first, then it changes to the maximum with the inverse bending curvature, and then it changes to a relatively small value as the inverse bending curvature becomes smaller, and the last few turns reverse the residual curvature until straightening.
- (2) The greater the inverse bending curvature, the faster the original curvature is unified. Conversely, the smaller the inverse bending curvature, the more the number of cornering required for the original curvature uniformity.
- (3) The greater the inverse bending curvature, the greater the overall deformation of the bar, and the deformation and deformation energy required for each bending will become larger. The large reverse bending curvature will result in a higher residual stress level on the bar after straightening. At the same time, a large reverse bending

curvature will increase the straightening force and also generate more energy consumption.

Considering the above factors, when selecting the variable curvature range required for the roll design, choose a smaller curvature in all curvature ranges that meet the straightening accuracy. Combined with the example in this project, considering that the straightening roll wear will cause the actual bending curvature to decrease, the radius of curvature is selected as  $1\rho_c \sim 0.5\rho_c$ .

### 5 Process parameter setting model

The technological setting parameters of two-roll straightener include concave roll angle, convex roll angle, roll gap, horizontal spacing of guide plate, and vertical distance of guide plate. The vertical distance of the guide plate is related to the vertical adjustment device of the guide plate on the equipment. The main requirement is to adjust the guide plate to the gap between the concave roll and the convex roll. This paper mainly describes the calculation and selection of concave roll angle, convex roll angle, roll gap, and guide plate spacing.

#### 5.1 Convex roll angle

After the roll shape is determined, the bending curvature of straightening bar is determined by the angle of concave roll and convex roll. In actual production, this angle

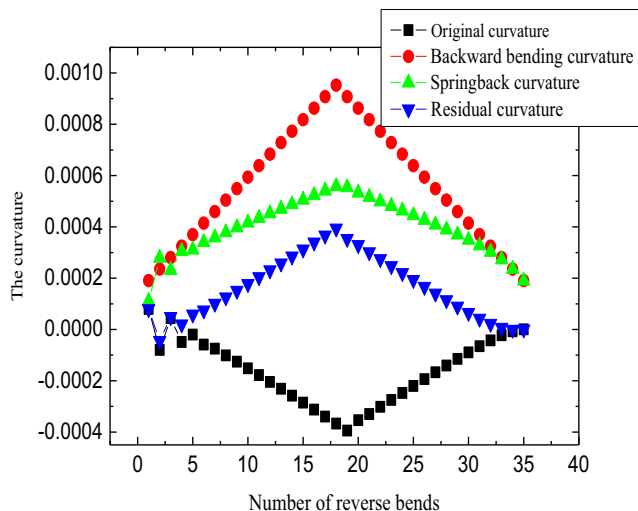


**Fig. 7** Curvature radius is  $1\rho_c \sim 0.2\rho_c$

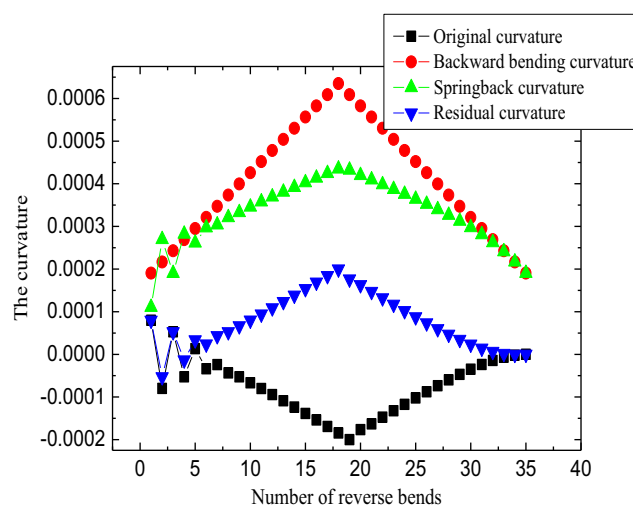


**Fig. 8** Radius of curvature is  $1\rho_c \sim 0.3\rho_c$



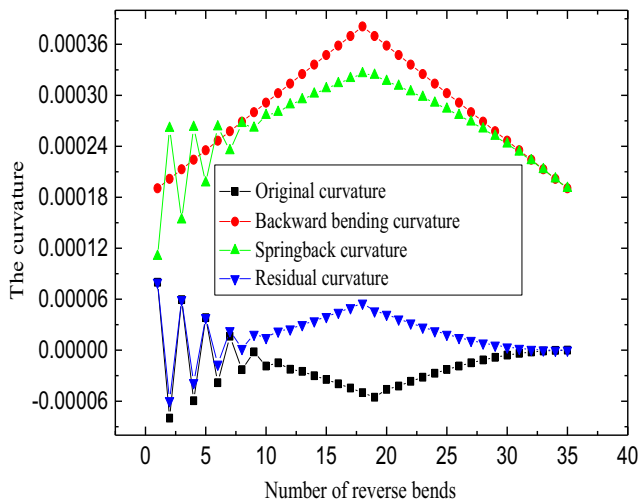


Fig. 9 Radius of curvature is  $1\rho_c \sim 0.5\rho_t$

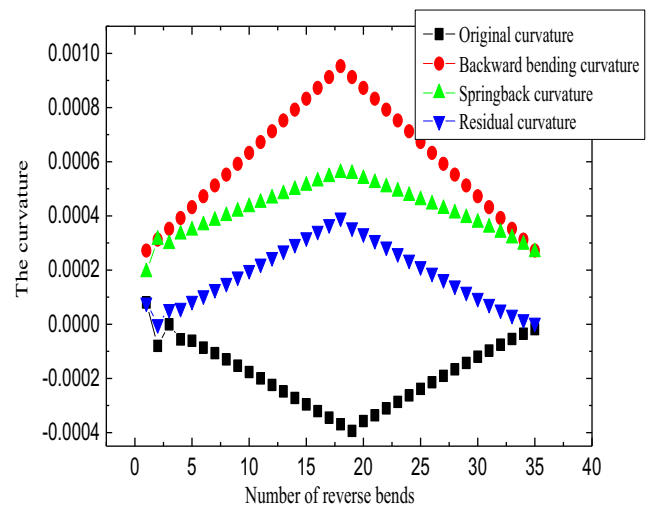


Fig. 11 Radius of curvature is  $0.7\rho_c \sim 0.2\rho_t$

determines the maximum bending shape of bar in roll gap, in which concave roll angle plays the most important role. In the roll gap setting model, the roll gap is required to restrict the bar completely (the gap effect in the tolerance range of bar diameter can be neglected). Therefore, it is approximated that the curve bending state obtained after the vertical surface of bar axis intersects with the concave roll is the action line of actual bending.

Iterative optimization method is used to solve the angle of concave roll, as shown in Fig. 12. Firstly, given the initial value of concave roll angle  $\alpha_1$  as the maximum allowable angle, a series of points on the intersection line between the vertical surface of bar axis and concave roll are obtained by curvature analysis method shown in Fig. 3. Based on these points, the curve equation of bending shape of bar in roll gap is obtained by spline function fitting method, and then the bending curvature at any point can be calculated. The residual curvature of bar with

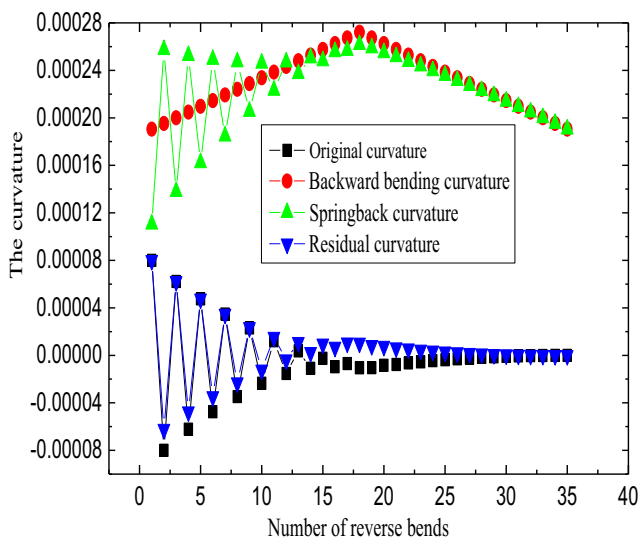


Fig. 10 Radius of curvature is  $1\rho_c \sim 0.7\rho_t$

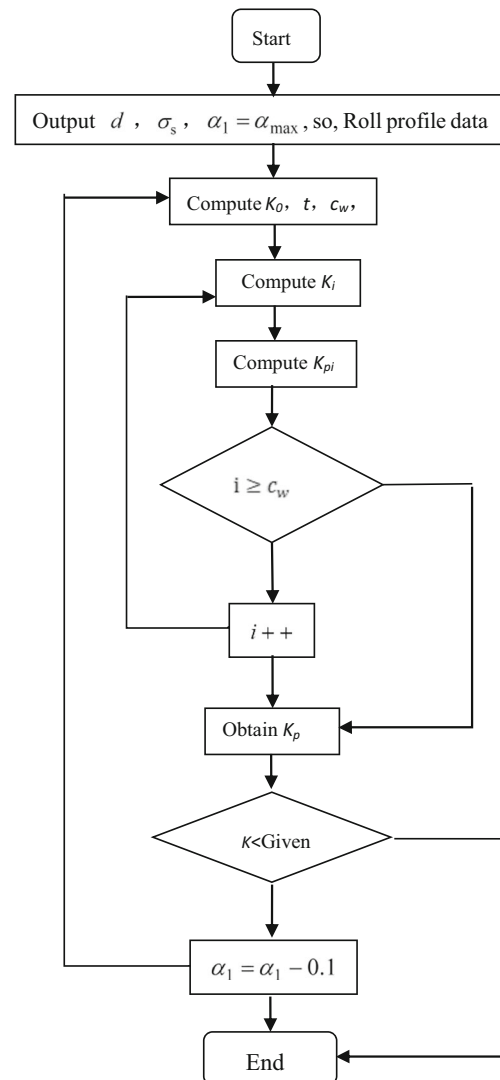
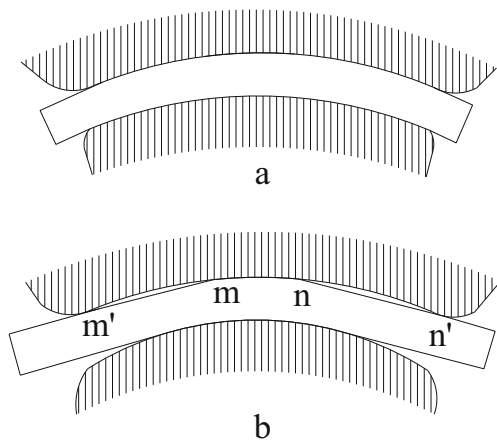


Fig. 12 Calculation of concave roll angle



**Fig. 13** Bar bending at different angles. Bar bending state (reasonable) (a). Bar bending state (unreasonable) (b)

concave roll angle  $\alpha_1$  can be calculated by iteration formula (Formula 20). If the straightening accuracy is satisfied, the angle is set as concave roll angle. Otherwise,  $\alpha_1$  will be reduced by 0.1 degrees and iterated again until the angle of concave roll that can straighten the bar is found.  $C_w$  is the total number of turns.

### 5.2 Convex roll angle

The angle of the convex roll acts as an auxiliary constraint. Its purpose is to make the bending state of the bar consistent with that of the concave roll in the vertical plane of the bar axis as far as possible, to minimize the length of the straight line segment of the bar in the roll gap and to reduce the blind zone. Figure 13a is the reasonable adjustment of the cam angle, the bending state of the bar is smooth, and Fig. 13b is the unreasonable adjustment of the cam angle. The  $m'$  and  $n'$  straight sections on the bar will produce blind areas.

In order to realize the reasonable adjustment of the angle of the convex roll, the geometric method is used to calculate iteratively to find the optimal angle of the convex roll.

**Table 2** Requirements for nominal dimensions of bar sections in national standards (mm)

Bar diameter/mm	Dimensional tolerance
$\Phi 5.5\sim 7$	$\pm 0.4$
$\Phi 7\sim 20$	$\pm 0.4$
$\Phi 20\sim 30$	$\pm 0.5$
$\Phi 30\sim 50$	$\pm 0.6$
$\Phi 50\sim 80$	$\pm 0.8$
$\Phi 80\sim 110$	$\pm 0.1$
$\Phi 110\sim 150$	$\pm 1.4$
$\Phi 150\sim 200$	$\pm 2$
$\Phi 200\sim 280$	$\pm 3$
$\Phi 280\sim 310$	$\pm 5$

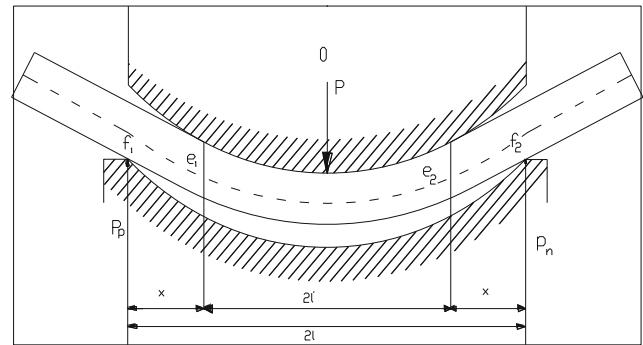


**Fig. 14** Bar and straightening roll contact state diagram

Firstly, the initial angle  $\alpha_2$  of the roll is given, and it is set to the adjustable maximum angle  $\alpha_{max}$ . By referring to the method in Fig. 12, the coordinate points on the intersection line between the convex roll and the vertical plane section where the bar axis is located (that is the bending action line of the convex roll to the bar) are obtained. The coordinate point abscissa spacing is the same as that obtained by concave roll. Then, the vertical distance between the corresponding coordinate points of the concave roll and the convex roll is calculated. If the vertical distance between each distance and the position of the roll waist is not very different, the angle adjustment is considered to be appropriate. Otherwise, let  $\alpha_2 = \alpha_2 - 0.1$  enter the next iteration until a reasonable roll angle is found.

### 5.3 Roll gap

The parameters of roll gap are the clearance between concave roll and convex roll waist. The ideal state of roll gap is that the clearance between concave roll and convex roll is equal to the diameter of bar, that is the straightening roll clamps bar without flattening. However, due to the tolerance of the bar, the value of roll gap in the process setting parameter module is the sum of the diameter of the bar and the upper deviation of the

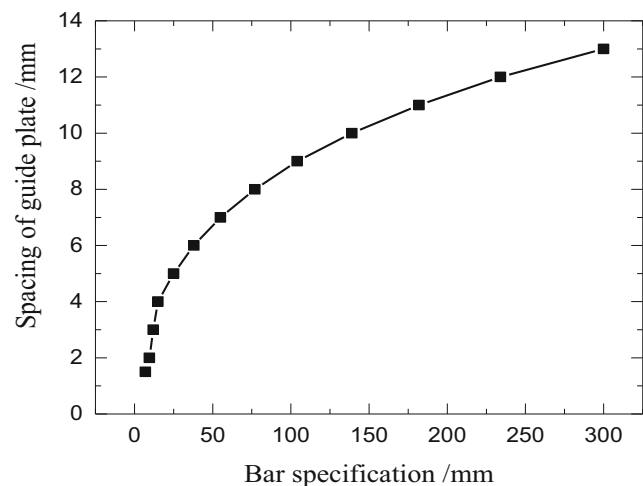
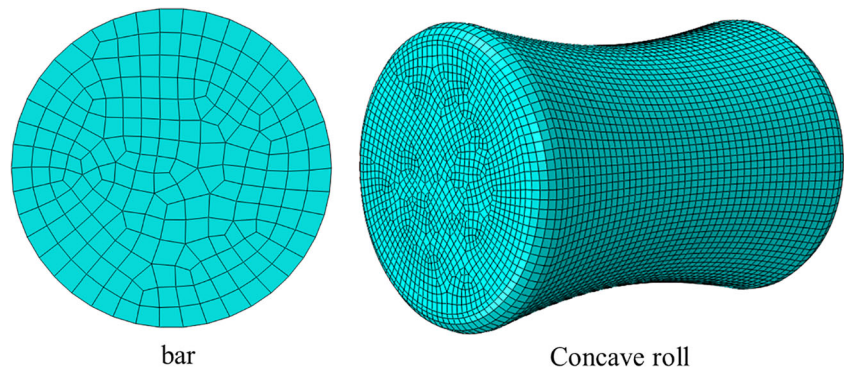


**Fig. 15** Rule of spacing of guide plate

**Table 3** Material properties of bars

Material	Modulus of elasticity	Poisson ratio	Yield strength	Strength limit	Elongation
16MnCr5	211 GPa	0.28	1187 MPa	1373 MPa	0.13

**Fig. 16** Cell partition mode



bar. Specific tolerance values are taken from national standard GB/T 702-2008 [23]. Table 2 shows the dimension deviation of bar sections with different specifications.

After setting the roll gap parameters, the actual size of the roll gap is related to the overall stiffness of the equipment and the wear of the roll system when the equipment is in operation. For the wear situation, it is necessary for workers to regularly check the difference between the set roll gap and the actual roll gap in order to compensate for the roll gap deviation caused by wear. For stiffness, the stiffness curve can be obtained by testing after the equipment is installed well, that is, the relationship between straightening force and elastic deformation. The elastic deformation can be compensated according to the value of the pressure sensor used to measure the straightening force.

It should be pointed out that when the setting value of roll gap is larger than the given value, the bar can also bend to a certain extent by adjusting the angle between concave roll and convex roll. As shown in Fig. 14, the purpose of straightening the bar can also be achieved. However, in this case, the bar is in contact with both ends of the concave roll (position  $f_1$  and  $f_2$ ) and with the middle position of the convex roll (section  $e_1e_2$ ). The bar with a large length in the roll gap is not directly restrained by the roll gap (section  $e_1f_1$  and  $e_2f_2$ ), so the head and tail of the bar cannot be straightened, and also, the straightening blind area is large (section  $e_2f_2$  or  $e_1f_1$ ). This is

the place that should be minimized in the process parameter setting of high-precision straightening.

**5.4 Spacing of guide plate**

The spacing of guide plate is the horizontal distance between the inner and outer guide plates, which plays the role of restraining the horizontal position of the bar. The smaller the spacing between guide plates, the tighter the bar restraint, the more stable the straightening, but the worse the wear will be. The specific value of the spacing of the new guide plate refers to the experience of the existing bar straightener in the factory. The specific value is shown in Fig. 15. Among them, the longitudinal coordinate is the clearance margin of guide plate; that is, the clearance margin of guide plate is the sum of the specification of bar and the given clearance margin. In addition, with the production going on, the guide plate will wear out. After wear, the set value of guide plate spacing needs to be gradually reduced to ensure stable straightening.

**6 Model validation**

In order to verify the correctness of the theoretical model, a finite element analysis was carried out on the straightening process of a two-roll straightener in a bar manufacturer.

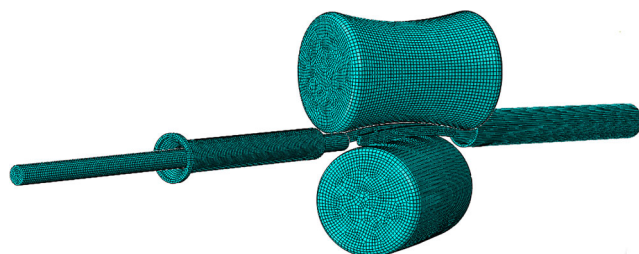


**Fig. 17** Finite element model

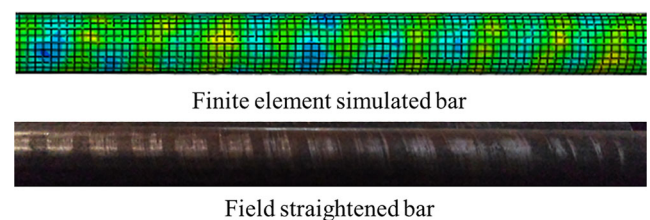
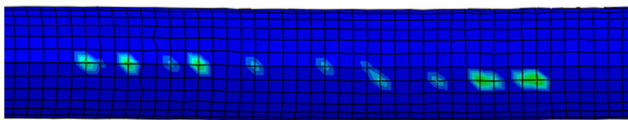
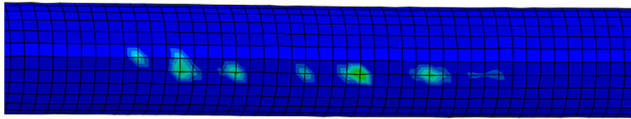


**Fig. 18** Comparison between the finite element model and field straightening



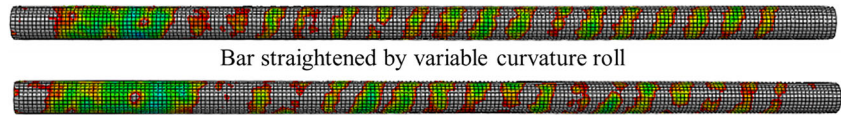
The contact state between the variable curvature roll and the bar



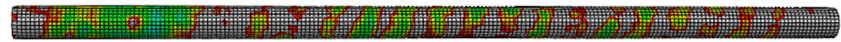
Contact state between straightening roller and bar in a factory

**Fig. 19** Comparison of contact states

**Fig. 20** Surface stress profile



Bar straightened by variable curvature roll



Bar after straightening of straightening roll in a factory



**Fig. 21** Straightener for a factory

The straightening process is analyzed by finite element method. The straightening roll, baffle, and sleeve are set as discrete rigid bodies in the model. The bar is set as deformable body. The model takes 16MnCr5 as an example. The material properties are shown in Table 3.

The finite element calculation process completely simulates the actual straightening process. Initial straightening rolls idle along their respective axes to ensure that the speed along the rolling direction is 25 m/min. The straightening roller has only rotational freedom and other directions are fixed. The baffles on both sides and the inlet and outlet sleeves are fixed. The contact between the bar and each straightening roller is surface to surface contact. Tangential friction coefficient is

0.2. The normal direction is the hard contact. There is no friction-free tangential contact between bar and baffle, inlet sleeve, and outlet sleeve, and the normal direction is hard contact, a total of 6 contact pairs. The linear hexahedral element C3D8R was selected for the bar element. The cell partition method is shown in Fig. 16, and the finite element model is shown in Fig. 17.

As shown in Fig. 18, by comparing with the field straightening process, it can be seen that the surface quality of the bar after the finite element simulation is similar to that of the bar after the field straightening, and has good straightness. The reliability of the finite element model is proved.

Then the finite element model is used to analyze the straightening process of the variable curvature roll. In this model, the number of variable curvature of roll shape is  $isn = 80$ , that is, 80-segment curvature. The finite element analysis of the two rolls is compared. Contact status is shown in Fig. 19. It can be seen that there are more contact points between the variable curvature roll and the bar; that is, the contact state is better. The stress distribution on the surface of bar is shown in Fig. 20. To make the contrast more obvious, the stress display range of finite element model is adjusted to 0–500 MPa. It can be seen that the stress distribution of the bar surface after straightening with variable curvature roller is more uniform.

At last, the roll shape of the two-roll straightener of a bar manufacturer was reformed. The straightener is shown in Fig. 21. The roll shape data are shown in Table 4, and the straightening test on site was carried out. The given target straightness



**Table 4** Data of the straightening roll type

Concave roll		Convex roll	
z/mm	R/mm	z/mm	R/mm
-185	130.17	-185	144.72
-172.6	129.93	-172.6	141.56
-160.3	129.75	-160.3	138.56
-148	129.62	-148	135.71
-135.6	129.54	-135.6	133.03
-123.3	129.5	-123.3	130.53
-111	129.49	-111	128.2
-98.67	129.52	-98.67	126.08
-86.33	129.57	-86.33	124.16
-74	129.64	-74	122.46
-61.67	129.71	-61.67	120.99
-49.33	129.79	-49.33	119.77
-37	129.87	-37	118.79
-24.67	129.94	-24.67	118.08
-12.33	129.98	-12.33	117.65

**Table 5** Site straightening parameters

Straightening parameter	Given value
Bar diameter/mm	Φ40
Bar yield strength/MPa	1000
Elastic modulus of material/MPa	206000
Hardening modulus of the material/MPa	50000
Angle of the concave roll/(°)	18.1
Angle of the convex roll/(°)	19.2
Spacing of guide plate/mm	46
Original deflection/(mm·m <sup>-1</sup> )	10
Length of roll profile/mm	400

is 0.6 mm·m<sup>-1</sup>. The process parameters of concave roll angle, convex roll angle, and guide plate spacing calculated from the process setting model in this paper are shown in Table 5. Because of the elastic deformation of the straightener, the parameters of roll gap are given according to the experience of setting the roll gap. Bar comparison after straightening on site is shown in Fig. 22.

The curvature variation of the whole straightening process is obtained by analytic calculation as shown in Fig. 23. The final residual curvature is 0.0000031667 and the corresponding deflection is 0.4 mm·m<sup>-1</sup>. The target results are consistent with the field straightening results.

**Fig. 22** Bar comparison after field straightening

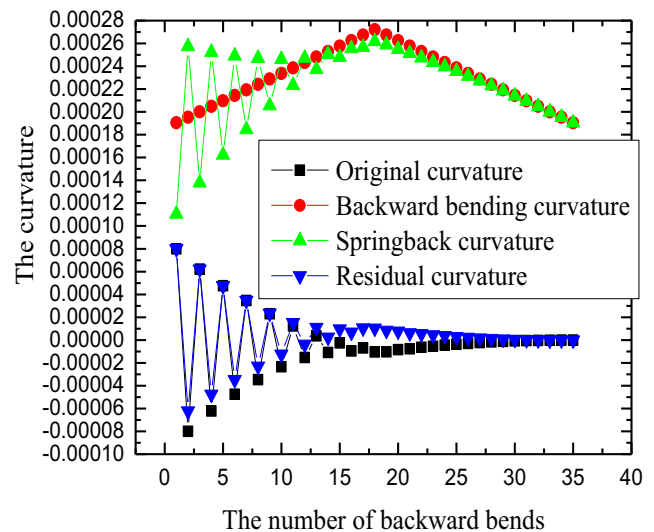
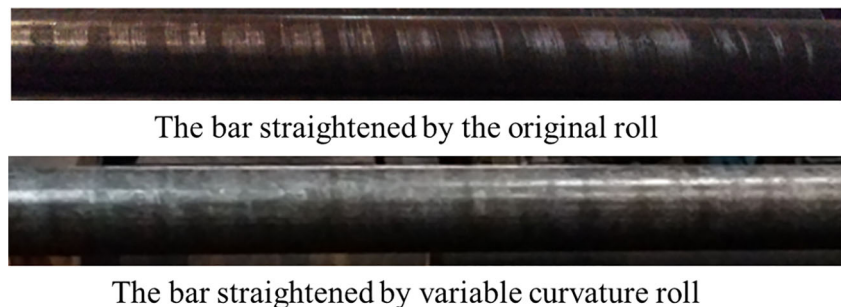


**Fig. 23** Curvature change process

### 7 Conclusion

The design method of variable curvature roll shape studied in this paper meets the requirements of curvature change and surface quality of bar in straightening. Based on the theory of small curvature plane bending springback theory, the curvature calculation process of elastic recovery in one bending of bar is deduced. According to the characteristic, every half circle of bar rotates corresponds to one reverse bending. The whole straightening process of bar is analyzed and calculated, and the optimization calculation of concave roll angle and convex roll angle is realized. On this basis, the setting method of the gap between rolls and guide plates is discussed, and the conclusions are as follows.

- (1) The roll shape design method based on uniform and variable curvature can be used to calculate the roll shape of two-roll bar straightening. The straightening roll designed with this roll shape can achieve high-precision straightening of bar.
- (2) The evolution process of original curvature, reverse curvature, springback curvature, and residual curvature under different curvature ranges can be obtained by the full process reverse bending springback calculation of bar



two-roll straightening. The influence of different curvature ranges on the final straightening accuracy of bar can be obtained by this method.

- (3) The concave roll angle and the convex roll angle need to be matched. The purpose is to make the bar reach a certain bending state in the roll gap and make the bending state as smooth as possible. The angle parameters obtained by the method described in this paper can meet the needs of straightening.
- (4) In the straightening process, the contact state between the variable curvature roller and the bar is good, and the surface quality of the bar can be improved.

**Acknowledgements** This work was supported by National Key R&D Program of China (grant number 2018YFB1308703), Major science and technology projects of Shanxi Province(20181102016)

## References

1. A.M. M (1979) Pipe straightener. The first section of heavy Research Institute, Xi'an, trans. Beijing: Mech Industry Press
2. Cui FM (2005) Straightening principle and straightening machine. Metallurgical Industry Press, Beijing
3. Pei YC, Wang JW, Tan QC, Yuan D Z, Zhang F. (2017) An investigation on the bending straightening process of D-type cross section shaft. *Int J Mech Sci* 131
4. Wu BJ, Chan LC, Lee TC, Ao LW. (2000) Study on the precision modeling of the bars produced in two cross-roll straightening. *J Mater Processing Tech* 99 (1):202–206
5. Yu GC, Zhao J, Ma R, Zhai RX (2016) Uniform curvature theorem by reciprocating bending and its experimental verification. *J Mech Eng* 52(18):57–63
6. Yu GC, Zhai RX, Zhao J, Ma R (2017) Theoretical analysis and numerical simulation on the process mechanism of two-roller straightening. *Int J Adv Manuf Tech* 1-11
7. Yu GC, Zhai RX, Zhao J, Ma R (2018) Theoretical analysis and numerical simulation on the process mechanism of two-roller straightening. *Int J Adv Manuf Tech* 94(9-12):4011–4021
8. Lu H, Ling H, Leopold J, Zhang X, Guo CQ. (2009) Improvement on straightness of metal bar based on straightening stroke-deflection model. *Sci China Ser E: Technol Sci* 52(7): 1866–1873
9. Wang CG, Yu GC, Wang W, Zhao J (2018) Deflection detection and curve fitting in three-roll continuous straightening process for LSAW pipes. *J Mater Process Tech* 255:150–160
10. Wang CG, Zhang ZY, Zhai RX, Yu GC, Zhao J (2018) Cross-sectional distortion of LSAW pipes in over-bend straightening process. *Thin-Walled Structures* 129:85–93
11. Zhao J, Yin J, Ma R, Ma LX. (2011) Springback equation of small curvature plane bending. *Sci China: Technol Sci* 54(9):2386–2396
12. Yin J, Zhao J, Wang SY, Wan XS. (2014) Principle of multi-roll straightening process and quantitative resolutions of straightening strategies. *J Iron Steel Res Int* 9(21):823–829
13. Wang YQ, Liu ZF, Luo YX, Yan XC. (2016) Curvature and residual stress analysis in rotational leveling of bars. *J Iron Steel Res Int* 23(7):669–676
14. Zhang ZQ, Yan YH, Yang HL (2013) The straightening curvature-radius model for the thin-walled tube and its validation. *J Mech Eng* 49(21):160–167
15. Zhang ZQ. (2016) Prediction of maximum section flattening of thin-walled circular steel tube in continuous rotary straightening process. *J Iron Steel Res Int* 23(8): 745–755
16. Zhang ZQ, Yan YH, Yang HL (2016) A simplified model of maximum cross-section flattening in continuous rotary straightening process of thin-walled circular steel tube. *J Mater Process Tech* 238:305–314
17. Zhao J, Song XK, Cao HQ, Liu J (2014) Principle of multi-point bending one-off straightening process for longitudinally submerged arc welding pipes. *J Mech Eng* 50(2):92–97
18. Moon C, Kim N. (2013) Dimensional change in drawn wire product in the two cross-roll straightening process. *Trans. Korean Soc. Mech. Eng. A* 37(3):295–302
19. Ma LF, Ma ZY, Jia WT, Lv YY, Jiang YP, Xu HJ, Liu PT (2015) Research and verification on neutral layer offset of bar in two-roller straightening process. *Int J Adv Manuf Tech* 79(9-12):1519–1529
20. Jindrich P, Tomas N, Frantisek Š (2016) Novel approach to computational simulation of cross roll straightening of bar. *J Mater Process Tech* 233:53–67
21. Li W, Lu C, Zhang J (2012) A local annular contrast based real-time inspection algorithm for steel bar surface defects [J]. *App Surf Sci* 258(16):6080–6086
22. Li W, Lu C, Zhang J (2013) A lower envelope Weber contrast detection algorithm for steel bar surface pit defects. *Optics & Laser Technology* 45:654–659
23. GB/T 702-2008 S Hot rolled round steel and square steel size and weight and tolerance

**Publisher's note** Springer Nature remains neutral with regard to jurisdictional claims in published maps and institutional affiliations.